HEALTH AND MEDICINE

Sutureless repair of corneal injuries using naturally derived bioadhesive hydrogels

Ehsan Shirzaei Sani[1]*, Ahmad Kheirkhah[2]*, Devyesh Rana[3], Zhongmou Sun[2], William Foulsham[2], Amir Sheikhi[4,5,6], Ali Khademhosseini[4,5,6,7], Reza Dana[2†], Nasim Annabi[1,4,6†]

Corneal injuries are common causes of visual impairment worldwide. Accordingly, there is an unmet need for transparent biomaterials that have high adhesion, cohesion, and regenerative properties. Herein, we engineer a highly biocompatible and transparent bioadhesive for corneal reconstruction using a visible light cross-linkable, naturally derived polymer, GelCORE (gel for corneal regeneration). The physical properties of GelCORE could be finely tuned by changing prepolymer concentration and photocrosslinking time. GelCORE revealed higher tissue adhesion compared to commercial adhesives. Furthermore, in situ photopolymerization of GelCORE facilitated easy delivery to the cornea, allowing for bioadhesive curing precisely according to the required geometry of the defect. In vivo experiments, using a rabbit stromal defect model, showed that bioadhesive could effectively seal corneal defects and induce stromal regeneration and re-epithelialization. Overall, GelCORE has many advantages including low cost and ease of production and use. This makes GelCORE a promising bioadhesive for corneal repair.

INTRODUCTION

More than 1.5 million new cases of corneal blindness are reported every year (*1*), of which only less than 5% are treated by corneal transplantations due to donor tissue shortage and the high expense of transplantation surgery (*2*). Corneal injuries and infections are common causes of corneal scarring and stromal thinning, which can lead to tissue and vision loss (*3*). In severe or progressive cases of corneal stromal inflammation, the stromal matrix may break down substantially to a point where the structure integrity of the eye is endangered. Current standards of care for treatment of corneal stromal defects include use of cyanoacrylate glue, tissue grafting, or corneal transplantation. However, these methods generally have significant drawbacks. For example, cyanoacrylate glue is associated with low biocompatibility, poor transparency, rough surface, difficult handling, and poor integration with corneal tissues (*4*, *5*). Grafting requires donor tissues, advanced surgical skills, and specialized equipment. Tissue grafting can also be associated with transplant rejection and suture-related complications such as cheese wiring through surrounding necrotic tissue, neovascularization, and microbial entrapment (*2*, *6*). Furthermore, using allogeneic tissue for grafting carries a high risk of immune reactions, specifically in those with acute injuries or infections (*7*). Considering the magnitude of this problem, coupled with the shortage of donor corneas worldwide, cost-effective and cell-free biomaterial implants are highly desirable clinically (*1*).

Adhesive biomaterials have risen as a promising approach for the treatment of corneal stromal loss, particularly in emergency situations. In general, biomaterials used for engineering corneal substitutes must use physical, structural, and physiobiological characteristics similar to the native cornea. An ideal biomaterial for corneal repair and regeneration must possess (i) biocompatibility and biodegradability, (ii) mechanical stability and appropriate stiffness, (iii) high transparency, (iv) high adhesion to the native tissue, (v) capability of cell support and endogenous tissue regeneration, and (vi) clinical compliance for ease of application and use (*8*).

Biomaterials used as tissue adhesives for corneal sealing and repair can be categorized into two classes: (i) synthetic adhesives [e.g., cyanoacrylates and polyethylene glycol (PEG)–based adhesives] and (ii) naturally derived adhesives (e.g., fibrin, polysaccharide, collagen-based adhesives, etc.) (*9*). Natural biopolymers tend to have excellent biocompatibility, but they often have low mechanical stability and adhesion. Synthetic biopolymers also enable customization of desired properties; however, they may not lead to tissue regeneration and biointegration (*8*). Currently, no available adhesive has been designed for long-term integration with the cornea even though significant research has been devoted to developing adhesives that can close corneal incisions (as opposed to "filling in" defects). For example, ReSure (Ocular Therapeutix Inc., MA, USA), a PEG-based adhesive, is the only U.S. Food and Drug Administration (FDA)–approved ocular sealant in the United States, which is designed to seal corneal incisions in cataract surgery (*5*). However, ReSure lacks the ability to fill stromal defects. It also has poor adhesion, especially in wet condition, and falls off quickly (*9*). OcuSeal (Beaver-Visitec International, MA, USA) is another PEG-based adhesive used in Europe for sealing corneal incisions, but it cannot be used for filling stromal defects, because of uncontrollable and rapid polymerization, which prevents sufficient time for thorough application (*10*). Li *et al.* also formulated a dual-thiol and acrylate gelatin-based hydrogel for ocular tissue regeneration; however, the use of ultraviolet (UV)–light cross-linking can cause corneal or retinal photochemical cytotoxicity or DNA damage (*11*, *12*). Other natural adhesives, including collagen vitrigel (*13*, *14*), fibrin (*15*), gelatin (GelFilm and GelFoam) (*16*), alginate (*17*), and chitosan (*18*) have also been developed for ocular regeneration applications. However, there is no existing hydrogel adhesive that combines both regenerative and adhesive properties and can properly mimic natural healing of corneal tissue (*5*). In addition, many of these biomaterials lack high adhesion

[1]Chemical and Biomolecular Engineering Department, University of California, Los Angeles, Los Angeles, CA, USA. [2]Massachusetts Eye and Ear Infirmary, Department of Ophthalmology, Harvard Medical School, Boston, MA, USA. [3]Department of Chemical Engineering, Northeastern University, Boston, MA, USA. [4]Biomaterials Innovation Research Center, Brigham and Women's Hospital, Harvard Medical School, Boston, MA, USA. [5]Department of Bioengineering, University of California, Los Angeles, Los Angeles, CA, USA. [6]Center for Minimally Invasive Therapeutics (C-MIT), California NanoSystems Institute (CNSI), University of California, Los Angeles, Los Angeles, CA, USA. [7]Department of Radiology, David Geffen School of Medicine, University of California, Los Angeles, Los Angeles, CA, USA.
*These authors contributed equally to this work.
†Corresponding author. Email: nannabi@ucla.edu (N.A.), reza_dana@meei.harvard.edu (R.D.)

to corneal tissue and long retention, appropriate optical properties (e.g., coloration and curvature), transparency, and proper stiffness required to fully integrate with the native cornea (*9*).

To address the unmet need of a biocompatible adhesive hydrogel for corneal tissue repair, we have engineered a gelatin-based adhesive biomaterial, GelCORE (gel for corneal regeneration), which can be used for quick and long-term repair of corneal stromal defects. The proposed bioadhesive hydrogel is made of a chemically modified form of gelatin and photoinitiators, which can be photocrosslinked after short-time exposure to visible light (450 to 550 nm). Upon completion of photocrosslinking, a solid and transparent hydrogel that firmly adheres to the corneal tissue is formed. The mechanical properties of the engineered hydrogel adhesives were optimized to mimic the stiffness of the native cornea. In addition, the adhesive formulations were modified to obtain high adhesion strengths to the cornea, while retaining appropriate biodegradability and high cytocompatibility in vitro. The adhesion characteristics of the bioadhesives were then tested on the basis of standard adhesion tests provided by American Society for Testing and Materials (ASTM) and compared to commercially available adhesives. Ex vivo tests on explanted rabbit eyes were also performed to evaluate the retention and burst pressures. Last, in vivo tests were conducted using a rabbit stromal cornea defect model to test the biocompatibility and retention of the biomaterial, as well as the corneal regeneration after bioadhesive application.

RESULTS

Synthesis and physical characterization of the adhesive hydrogels

We synthesized a transparent, flexible, and adhesive photocrosslinkable hydrogel for the treatment of corneal stromal defects. The engineered hydrogel mimicked the mechanical properties of the native cornea and comprised a chemically modified form of hydrolyzed collagen, which provides enzymatic degradation sites and physiological cell adhesion motifs (*19*). UV cross-linkable gelatin-based sealants for sealing and repair of lung tissues (*19*) and sclera (*11*) have been reported. However, the use of UV light can induce DNA damage (*20*) and can cause corneal or retinal photochemical toxicity (*21*, *22*), as well as carcinogenesis (*23*). Specifically, UV-A (the longer wavelength) can cause retinal damage deeper within the eye (i.e., macular degeneration), and UV-B (the shorter wavelength) can cause damage to the surface of the eye (i.e., photokeratitis or corneal sunburn) (*24*). This limits the use of UV-mediated cross-linking techniques for corneal repair. To overcome the biosafety concerns associated with UV-initiated cross-linking, we investigated a visible light cross-linking system to form GelCORE adhesives, where light intensity is well under the maximum permissible exposure limit (*25*). In our work, the adhesive hydrogels could be cross-linked through a free radical polymerization process, in the presence of a type 2 initiator Eosin Y, as well as triethanolamine (TEA) and *N*-vinylcaprolactam (VC) as co-initiator and co-monomer, respectively (Fig. 1A).

The visible light cross-linking scheme has been proven to improve cell viability, compared to UV cross-linked systems (*26*–*28*). Briefly, the visible light photons excite the photoinitiator molecules (Eosin Y) to a triplet state, which allow them to accept hydrogen atoms from co-initiator molecules (TEA). The deprotonated radicals then undergo vinyl-bond cross-linking with co-monomer (VC) via chain polymerization. This will result in accelerated gelation of the polymeric scaffolds (*29*). This visible light photocrosslinking chemistry is an FDA-approved system (*30*) and has been used previously as a safe photocrosslinking system for biomedical applications (*29*, *31*, *32*). A schematic of the polymer network photocrosslinking process with representative images of the cross-linked adhesive on a corneal defect are shown in Fig. 1B. The hydrogel prepolymer solution could be easily and rapidly applied to a corneal stromal defect and photopolymerized, allowing the defects with varied shapes and sizes to be quickly sealed and thus promoting regeneration of new stromal tissue (Fig. 1, B to D). Accordingly, after creation of corneal stromal defect (Fig. 1Bi), the GelCORE prepolymer is applied to fill the defect site (Fig. 1Bii). Next, in the early stages of the healing process, the corneal epithelial layer begins to regenerate (Fig. 1Biii), and the full stromal regeneration occurs at the late repair process (Fig. 1Biv).

To determine the cross-linking density of the hydrogel network, 500-MHz proton nuclear magnetic resonance (^{1}H NMR) analysis was performed on GelCORE prepolymers and GelCORE hydrogels photocrosslinked at 1-, 2-, and 4-min visible light exposure times using techniques previously defined (fig. S1) (*32*). Results showed that methacryloyl (methacrylate/methacrylamide, –C=CH_2) functional groups in the GelCORE backbone with characteristic peak 1 at δ = 5.3 parts per million (ppm) and peak 2 at δ = 5.7 ppm were incorporated in the formation of the cross-linked three-dimensional (3D) bioadhesive network. Accordingly, the degree of cross-linking could be calculated by measuring the alteration in integrated areas of the methacryloyl peaks before and after the photocrosslinking process (*32*). On the basis of our results, it was found that the degree of cross-linking increased from 63.4 ± 2.7% to 88.9 ± 7.9% when visible light exposure time was increased from 1 to 4 min for 20% GelCORE concentration (fig. S2). Comparatively, we previously reported the formation of a UV–cross-linkable gelatin-based hydrogel as a lung sealant, which demonstrated >95% cross-linking density after 3-min UV exposure time (*19*).

Physical properties (i.e., mechanical properties, in vitro swelling ratio, and degradability) of GelCORE adhesive hydrogels were characterized. Mechanical properties of the bioadhesives were determined through compression and tensile tests (Fig. 1, E to G). Our results revealed that by varying the concentration of GelCORE and the photocrosslinking time, the critical mechanical properties of the hydrogel could be finely controlled to derive formulations with tensile and compressive moduli that are comparable to the native cornea (Fig. 1, E to G). For instance, the compressive modulus of adhesive hydrogels engineered with 5% (w/v) GelCORE increased from 1.2 ± 0.5 kPa to 4.5 ± 1.2 kPa as the light exposure time increased from 1 to 4 min, respectively (Fig. 1F). In addition, increasing the prepolymer concentration remarkably enhanced the mechanical properties of the bioadhesives. For instance, the compressive modulus of hydrogels formed by using 4-min light exposure time was increased 66.4-fold from 4.5 ± 1.2 kPa for 5% polymer concentration to 299.9 ± 30.0 kPa for 20% polymer concentration (Fig. 1F). This highlights the wide range of controllable moduli, which can be obtained just by changing either polymer concentration or photocrosslinking time. Comparatively, the compressive moduli of the adhesive hydrogels were well encompassing of the range of moduli of native cornea (115.3 ± 13.6 kPa), which is crucial for long-term tissue/biomaterial integration and remodeling (Fig. 1F). Rizwan *et al.* (*33*) formed UV cross-linked gelatin-based hybrid patches for corneal tissue regeneration with similar compressive moduli (ranged from 28.8 to 233.3 kPa) when the total polymer concentration changed from 10 to 30% (w/v). However, the application of this prefabricated graft required advanced surgical skills and equipment (*33*).

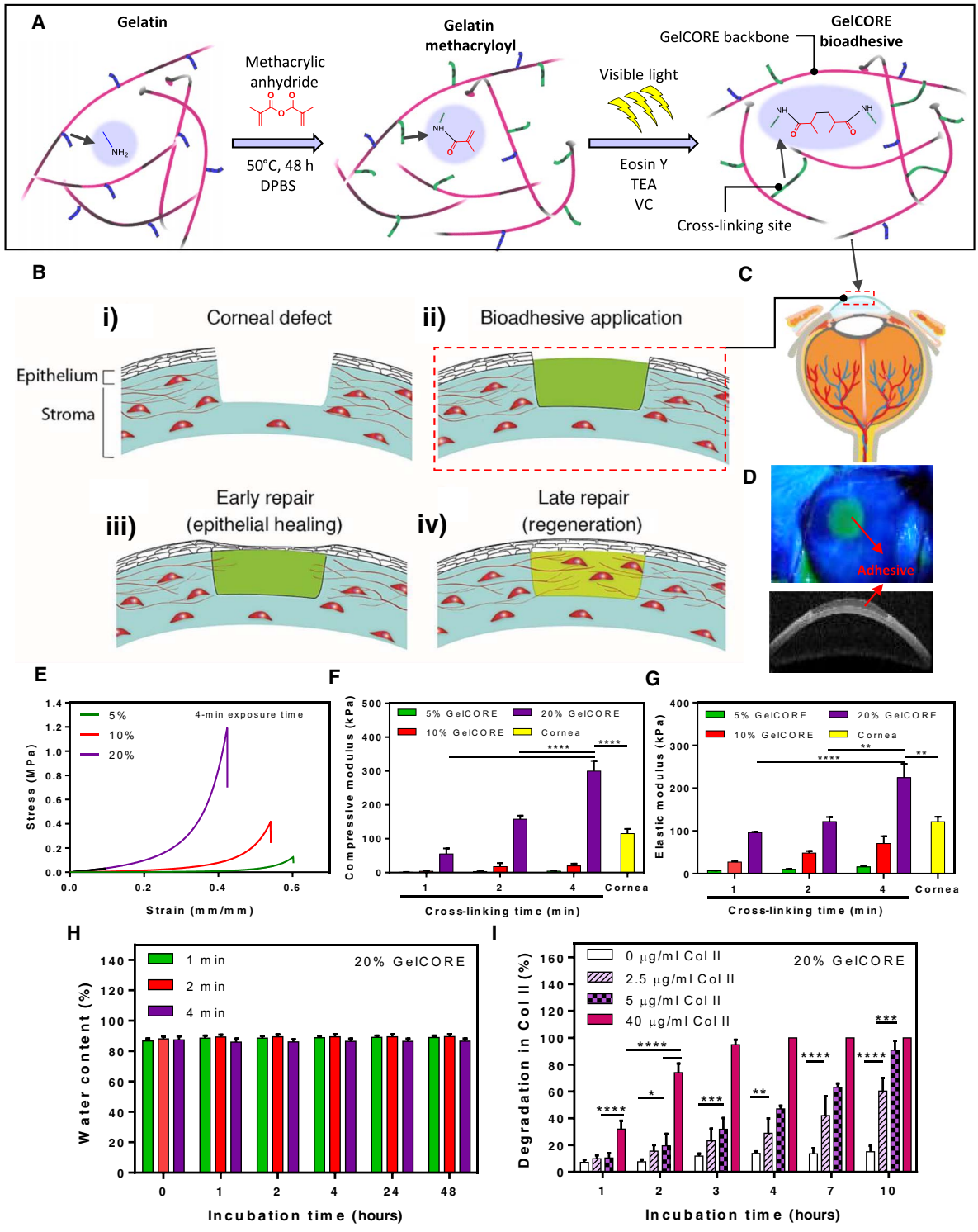

Fig. 1. Synthesis, application, and in vitro characterization of GelCORE adhesive hydrogels. (**A**) Schematic of the chemical reaction for GelCORE formation and photocrosslinking of the prepolymer solution with Eosin Y (photoinitiator), TEA (co-initiator), and VC (co-monomer). (**B**) Schematic diagram for the application of GelCORE for rapid and long-term repair of corneal injuries, which include (i) formation of stromal defect, (ii) application of the bioadhesive, (iii) regeneration of the epithelial layer, and (iv) stromal regeneration. (**C**) The prepolymer solution is injected into the corneal defect and exposed to visible light, forming (**D**) an adhesive GelCORE hydrogel. (**E**) Representative compressive stress-strain curves, (**F**) compressive moduli, and (**G**) elastic moduli of GelCORE adhesive hydrogels fabricated using 5%, 10%, and 20% (w/v) total polymer concentrations with varying photocrosslinking time points. (**H**) Water content of GelCORE adhesives produced by using 20% (w/v) polymer concentration and varying visible light exposure times at 37°C in DPBS over time. (**I**) In vitro degradation of 20% (w/v) GelCORE adhesive (4-min photocrosslinking time), in different concentrations of collagenase type II (Col II) solution in DPBS and 37°C over time. All hydrogels were polymerized by using 0.1 mM Eosin Y, 1.5% (w/v) TEA, and 1% (w/v) VC in distilled water. Data are reported as means ± SD (*P < 0.05, **P < 0.01, ***P < 0.001, and ****P < 0.0001; $n \geq 3$).

Similarly, tensile tests on GelCORE bioadhesives revealed tunable elastic moduli (Fig. 1G) and ultimate tensile strength (UTS) (fig. S3) by varying the GelCORE concentration and visible light exposure time. For example, the Young's moduli of adhesive hydrogels engineered with 5% (w/v) GelCORE enhanced from 6.7 ± 0.8 kPa to 16.0 ± 2.1 kPa by increasing the photocrosslinking time from at 1 to 4 min (Fig. 1G). In addition, the Young's moduli of the adhesive hydrogels photocrosslinked at 4 min increased 14-fold from 16.0 ± 2.1 kPa to 224.4 ± 32.3 kPa by increasing the total polymer concentration from 5 to 20% (w/v) (Fig. 1G). Furthermore, the UTS of engineered bioadhesives was consistently increased from 38.0 ± 6.1 kPa to 45.3 ± 4.1 kPa for 20% (w/v) GelCORE, when the photocrosslinking time increased from 1 to 4 min (fig. S3). Similar to compressive tests, these results demonstrated that the elastic moduli of the GelCORE bioadhesives were in the range of native corneal tissue (121.8 ± 11.6 kPa) (Fig. 1G). This enhancement in stiffness of the hydrogels at higher polymer concentrations or light exposure time can be due to the higher cross-linking density within the hydrogel network as confirmed by ^{1}H NMR analysis.

In addition to mechanical properties, water content and enzymatic degradation of the engineered adhesive hydrogels were also characterized. The degree of hydration (water content) of the GelCORE adhesives was measured in Dulbecco's phosphate-buffered saline (DPBS) (37°C, 48 hours). After 48 hours of incubation, no significant differences were observed in the water content of the GelCORE samples synthesized at 1-, 2-, and 4-min photocrosslinking time. In addition, the degree of hydration did not alter by time, when incubated for 48 hours in DPBS (37°C). Furthermore, the water content of the samples was in the range of 85.9 to 89.5% (Fig. 1H), which was found to be comparable to the degree of hydration of the native human cornea (85 to 86%) (*34*).

The enzymatic degradations of photocrosslinked GelCORE hydrogels were measured by incubating them in different concentrations (0, 2.5, 5, and 40 μg/ml) of collagenase type II solution in DPBS for up to 10 days (Fig. 1I). Results showed that the enzyme concentration could directly affect in vitro degradation rate of the hydrogels. For example, the adhesives showed 100% degradation after 4 days of incubation at the highest enzyme concentration (40 μg/ml). However, 13.8 ± 1.6%, 28.9 ± 11.1%, and 46.9 ± 2.4% degradations were obtained after 4 days, when the samples were incubated in different enzyme concentrations (0, 2.5, and 5 μg/ml, respectively) (Fig. 1I). Moreover, the degradation rate of 20% (w/v) GelCORE bioadhesives increased from 15.1 ± 4.3% to 90.7 ± 7.0% by increasing enzyme concentration from 0 to 5 μg/ml after 10 days of incubation (Fig. 1I). The ability to control and tune the degradation rates of the hydrogels is remarkably advantageous for the implementation of GelCORE as an adhesive for ocular applications. This can promote simultaneous bioadhesive enzymatic degradation and tissue integration, which can result in the new corneal stromal tissue ingrowth.

Overall, the physical characterization of GelCORE adhesive hydrogels demonstrated that the mechanical properties and in vitro enzymatic degradation can be tuned by changing total polymer concentration and photocrosslinking time. This significant degree of tunability suggests that the GelCORE bioadhesive could be readily adjusted for various surgical and tissue engineering applications, especially regeneration of corneal stroma defects.

In vitro adhesion properties of GelCORE bioadhesives

In general, high adhesion of hydrogels to the adjacent tissue can avoid biomaterial detachment from target tissues in vivo and eventually promote potential biointegration. An ideal tissue and biomaterial integration improves biocompatibility and enhances tissue regeneration under physiological conditions (*35*). Herein, we examined critical properties for effective bioadhesion, including shear strength, adhesion strength, and burst pressure, according to ASTM standards for biological adhesives. In these standards, the in vitro adhesion strength and sealing properties of GelCORE adhesive hydrogels, produced at various prepolymer concentrations and visible light exposure times, were compared to commercial surgical sealants, Evicel and CoSEAL (Fig. 2).

To investigate burst pressures of the engineered adhesives, air was continuously pumped into a custom-designed burst pressure apparatus. The adhesive polymers were applied to seal a standardized defect in a porcine intestine sheet as a biological substrate, based on a modified ASTM standard test, F2392-04 (Fig. 2A). The sealed tissue es then placed in the burst pressure apparatus. Our results showed that the burst pressures of GelCORE adhesives significantly increased from 10.8 ± 1.6 kPa to 63.1 ± 8.5 kPa as the GelCORE concentration was increased from 5% (w/v) to 20% (w/v) at 4-min photocrosslinking time (Fig. 2B). Comparatively, Gratieri *et al.* (*18*) reported burst pressures of approximately 12 kPa for a chitosan-based adhesive for ocular regeneration. This value is significantly lower than GelCORE-based adhesives presented here. Furthermore, cyanoacrylate glues for corneal repair showed burst pressure of approximately 68 kPa, which is comparable to our engineered adhesives (*36*). However, cyanoacrylate glues are generally toxic and show low biocompatibility and poor transparency (*4*, *5*). Moreover, a UV–cross-linkable gelatin-based adhesive used for ocular application achieved maximum a burst pressure of around 12 kPa as well (*36*, *37*), which is below the value obtained for GelCORE adhesives [~58 to 63 kPa for 20% (w/v) polymer concentration at 1- to 4-min light exposure time, respectively]. Furthermore, burst pressures of GelCORE adhesive hydrogels in all tested concentrations [5, 10, and 20% (w/v)] were significantly higher than both clinically available sealants, with a range of 11.1 ± 0.6 kPa to 63.1 ± 8.5 kPa as compared to 1.5 ± 0.7 kPa for Evicel and 1.6 ± 0.2 kPa for CoSEAL (Fig. 2B). GelCORE adhesive hydrogels additionally showed higher burst pressures than values of 0.3 ± 0.3 kPa for CoSEAL, as reported by Campbell *et al.* (*38*). Furthermore, our GelCORE adhesive achieved higher burst pressures than DuraSeal (0.8 kPa) and fibrin sealant (0.2 kPa) (*38*). In addition, it was reported that majority modes of failure for these commercial products were related to the cohesive properties of the materials (*38*). This indicates that these bioadhesives were inherently weak. It should be noted that burst pressure values for 20% GelCORE sealant were not significantly improved when increasing the photocrosslinking time from 1 to 4 min (Fig. 2B).

Next, the shear strengths of the engineered bioadhesives were investigated using a modified test based on ASTM standard F2255-05 (Fig. 2C). Similar to the burst pressure results, a wide range of shear stresses were obtained, indicating fine controllability and repeatability of shearing properties. The highest shear strength was observed for a 20% (w/v) GelCORE bioadhesive (375.2 ± 28.0 kPa) at 4-min photocrosslinking. This value was significantly higher than the lap shear strength of Evicel (207.7 ± 67.3 kPa) and CoSEAL (69.7 ± 20.6 kPa) (Fig. 2D). Moreover, increasing the photocrosslinking time from 1 to 4 min improved the shear strength of GelCORE adhesives for all tested concentrations. For example, the shear strength of 10% (w/v) GelCORE adhesive increased from 15.6 ± 2.9 kPa to 246.5 ± 12.6 kPa by increasing photocrosslinking time from 1 to 4 min as shown in Fig. 2D.

Last, the adhesion strengths of the engineered adhesives were investigated using a modified wound closure test based on ASTM standard F2458-05 (Fig. 2E). Similarly, a higher adhesive strength was

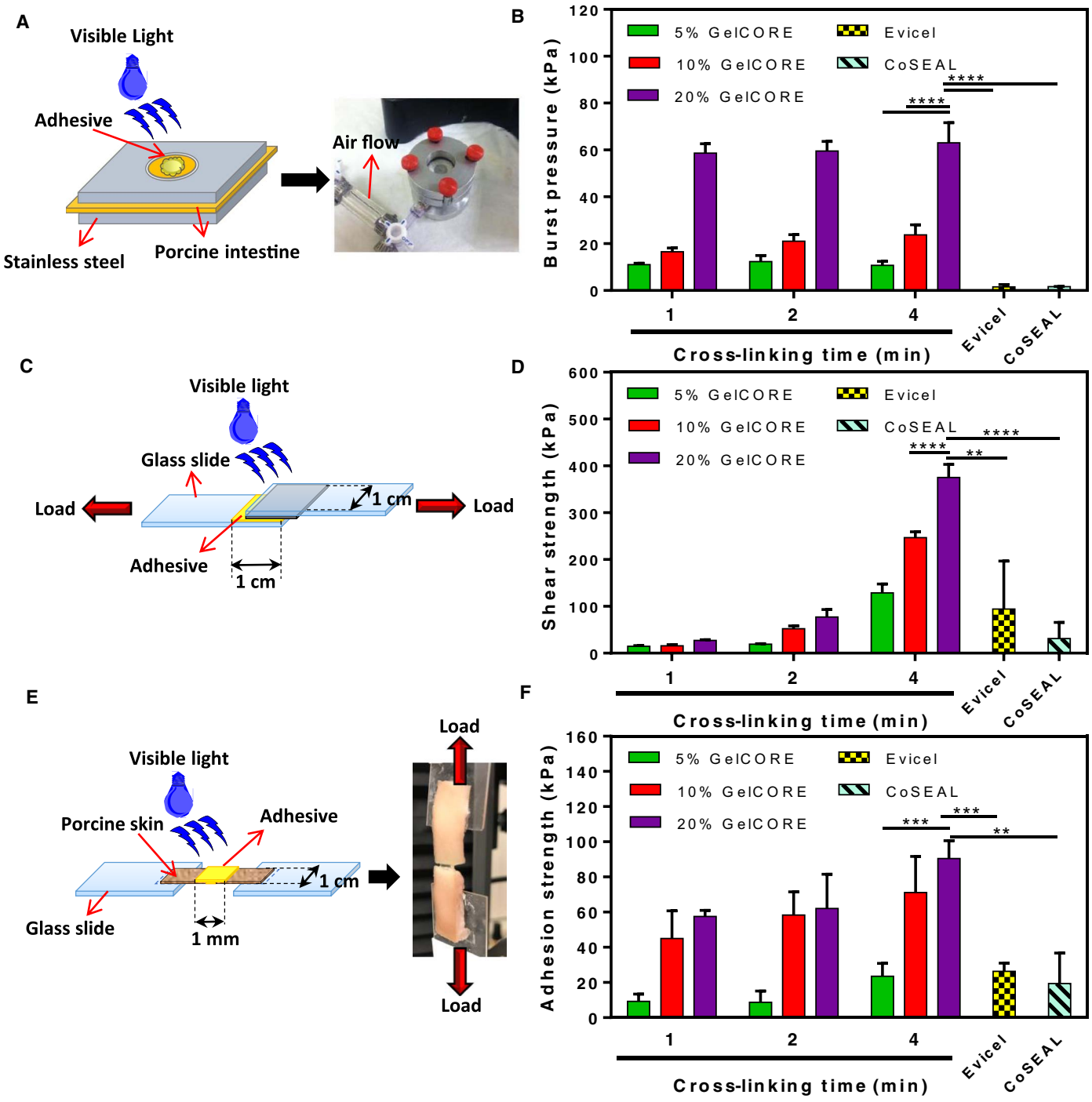

Fig. 2. In vitro adhesion properties of GelCORE hydrogels using porcine skin and intestine as biological substrates. (**A**) Schematic of the modified test for burst pressure measurements (ASTM F2392-04) and (**B**) average burst pressure of GelCORE adhesives ($n \geq 3$) produced with varying polymer concentrations and photocrosslinking times, compared to two commercial adhesives including Evicel and CoSEAL. (**C**) Schematic of the modified test for lap shear strength measurements (ASTM F2255-05) and (**D**) average shear strengths of GelCORE adhesives ($n \geq 3$) produced with varying polymer concentrations and photocrosslinking times, Evicel, and CoSEAL. (**E**) Schematic of the modified test for wound closure test (ASTM F2458-05) and (**F**) average adhesive strengths of GelCORE adhesives ($n \geq 3$) produced with varying polymer concentrations and photocrosslinking times, compared to Evicel and CoSEAL. Data are means ± SD (*$P < 0.05$, **$P < 0.01$, ***$P < 0.001$, and ****$P < 0.0001$). (Photo credit: Ehsan Shirzaei Sani, UCLA)

observed at higher concentration of GelCORE. For example, 20% GelCORE hydrogels, cross-linked via 4-min visible light exposure, reached an adhesive strength of 90.4 ± 10.2 kPa. This value was remarkably higher than that of CoSEAL (19.4 ± 17.3 kPa) and Evicel (26.3 ± 4.7 kPa) (Fig. 2F). This was also higher than adhesive strengths obtained by other commercially available bioadhesives or sealants such as Quixil (24.6 kPa), Beriplast (24.2 kPa), Tachosil (59.6 kPa), and Tisseel (77.5 kPa) (*39*). In addition, it was found that the adhesive strengths of the engineered GelCORE adhesives were also affected by the light exposure time. For example, adhesion strengths

increased from 57.5 ± 3.5 kPa to 90.4 ± 10.2 kPa as exposure time was increased from 1 to 4 min for a 20% GelCORE hydrogel (Fig. 2F).

Overall, the measurement of mechanical and adhesive properties of GelCORE adhesives showed excellent cohesion and adhesion for 20% GelCORE concentration. The wound closure strength, shear resistance, and burst pressure for a 20% (w/v) GelCORE bioadhesive were significantly higher than clinically available PEG-based (Evicel) and fibrin-based (CoSEAL) controls.

Ex vivo retention and burst pressure of the GelCORE bioadhesive

Dimensional stability and retention time for GelCORE bioadhesives were investigated on corneal tissues ex vivo by using slit lamp biomicroscopy and anterior segment optical coherence tomography (AS-OCT) (Fig. 3). Upon creation of a corneal defect in explanted New Zealand rabbit eyes (3 mm in diameter and >50% deep), the adhesive precursor solutions [10 and 20%(w/v)] were applied to the defect site and exposed to visible light for 1, 2, and 4 min, forming a transparent hydrogel with a smooth surface and complete corneal curvature (Fig. 3A). The GelCORE hydrogel could strongly adhere to the explanted tissue (movie S1). After application of the bioadhesives, eyes sealed with hydrogels were stored in DPBS at 4°C, and changes in bioadhesive structure and retention were assessed over time using serial evaluations with slit lamp biomicroscopy and AS-OCT (Fig. 3, A to C). Upon observation, all examined hydrogels showed firm adhesion to the corneal stroma. In addition, results revealed that retention times for 10 and 20% (w/v) GelCORE at 4-min photocrosslinking times were 15 and 17 days, respectively. This was 2.1 and 2.5 times higher than the retention times for 20% GelCORE formed at 1-min exposure time, respectively (Fig. 3B). This observation can be correlated to higher adhesion strengths of 10 and 20% (w/v) GelCORE adhesives at 4 min exposure time based on the wound closure test (Fig. 2F). It was also noted that for the duration of a 20-day assessment period, the bioadhesives remained uncompromised (thickness and spread were fully retained), and the adhesives were completely attached to the cornea in all tested eyes (Fig. 3C). Slit lamp biomicroscopy also corroborated that during this time period, the bioadhesive remained transparent with a smooth surface without any microscopic signs of changes in shape or contour. AS-OCT also confirmed no change in thickness or shape of the bioadhesive after 28 days (Fig. 3C).

An ex vivo burst pressure test was also performed to measure the burst pressures of bioadhesives on rabbit eyes (Fig. 3D). Accordingly, a 2-mm full-thickness incision was created in the cornea, followed by sealing with either GelCORE bioadhesives or ReSure (as control). For this test, GelCORE adhesive precursors and ReSure were applied to the corneal incision sites in explanted rabbit eyes and cross-linked in situ. The sealed eye was then connected to a burst pressure apparatus containing a syringe pump and a pressure sensor. Air was injected continuously, increasing pressure until bursting of the sealant (Fig. 3D). Burst pressures of explanted eyes sealed with 20% GelCORE adhesives engineered at varying visible light exposure times (1, 2, and 4 min) were measured using a digital wireless sensor (Fig. 3E). Burst pressures of the GelCORE adhesives formed at 4-min photocrosslinking were found to be 30.1 ± 4.3 kPa. This was approximately 10 times higher than that of normal eye pressure and significantly higher than burst pressure of the commercial control, ReSure (15.4 ± 6.3 kPa) (Fig. 3E). Last, by increasing the photocrosslinking time from 1 to 4 min, burst pressures of 20% (w/v) bioadhesives increased from 10.4 ± 1.5 to 30.1 ± 4.3 kPa (Fig. 3E).

Inclusively, the adhesive hydrogels engineered by using 20% GelCORE and photocrosslinked by using 4-min exposure time showed the highest ex vivo burst pressure resistance and retention time. Therefore, this hydrogel formulation was selected for in vitro cell studies and in vivo assessment of bioadhesive retention and cornea tissue regeneration.

In vitro assessment of cytocompatibility and integration of GelCORE bioadhesive

The optimal bioadhesive for corneal repair should be biocompatible with no cytotoxicity. It should also permit cells of the injured tissue to migrate into the bioadhesive for long-term integration and repair. Therefore, we aimed to evaluate the in vitro cytocompatibility and cell migration for the engineered adhesives using 2D cell seeding and scratch tests (Fig. 4).

To accomplish this, cytocompatibility of engineered bioadhesives was assessed in vitro. The viability, adhesion, proliferation, and metabolic activity of human cornea fibroblast cells (keratocytes) seeded on GelCORE adhesives were evaluated by using a commercial kit for LIVE/DEAD assay and PrestoBlue tests. In addition, the results were compared to viability and methanolic activity of the cells seeded on tissue culture well-plates and ReSure sealant as controls. The results showed that the cells seeded on both tissue culture well-plate control and bioadhesives (20% GelCORE) exhibited high viability (>90%) 1, 4, and 7 days after seeding (Fig. 4, A to B and D). In contrast, the cell viability for ReSure sealant was significantly lower than GelCORE adhesive (<65%) during the same time period (Fig. 4, C and D). The quantification of cell metabolic activity also confirmed this observation, where the metabolic activity of keratocytes seeded on ReSure was 1.2- and 2.8-fold lower than the cells seeded on GeCORE adhesive on days 1 and 7 after seeding (Fig. 4E). In addition, metabolic activity of keratocytes seeded on GelCORE adhesive increased consistently from 4008 ± 1795 relative fluorescence units (RFUs) at day 1 to 31,139 ± 697 RFUs at day 7 after seeding, respectively (Fig. 4E). Furthermore, actin/4′,6-diamidino-2-phenylindole (DAPI) staining exhibited an increase in cell spreading on the GelCORE bioadhesive over time (fig. S4).

The in vitro scratch assay also revealed that keratocytes seeded on the surface of both well plate and adhesive hydrogels could migrate to the scratched area (400- to 500-μm distance) in less than 24 hours (Fig. 4, F and G). In addition, to quantify the migration to the wound area, we compared cell density in the scratched area to the surrounding cell density. The results showed that the relative cell density for GelCORE adhesive hydrogels was significantly higher than that of the control (tissue culture plate) 1, 2, and 3 days after creating the scratch (Fig. 4H). For example, the relative cell density for GelCORE hydrogel was 94.4 ± 3.4%, which was 36% higher than the control (well plate). This indicates that cell migration and proliferation on the surface of GelCORE adhesives were higher than that of the control (Fig. 4H).

Many researchers investigated cytotoxicity and biocompatibility of synthetic bioadhesives and sealants in vitro and in vivo, and the cytotoxic nature of some of the synthetic bioadhesives has been widely reported (*9*, *40*–*42*). For example, Chen *et al.* (*40*) reported high levels of corneal cytotoxicity for methoxypropyl cyanoacrylate and *N*-butyl cyanoacrylate, while fibrin glue showed minimal cytotoxicity in their studies. However, cyanoacrylate-based adhesives showed a higher capability to seal corneal incisions compared with fibrin glue. In another study, Fürst and Banerjee (*41*) showed high in vitro and in vivo toxicity of BioGlue, which is a sealant based on bovine serum albumin and glutaraldehyde cross-linker. Their results revealed that cross-linked BioGlue released significant amounts of glutaraldehyde that can cause

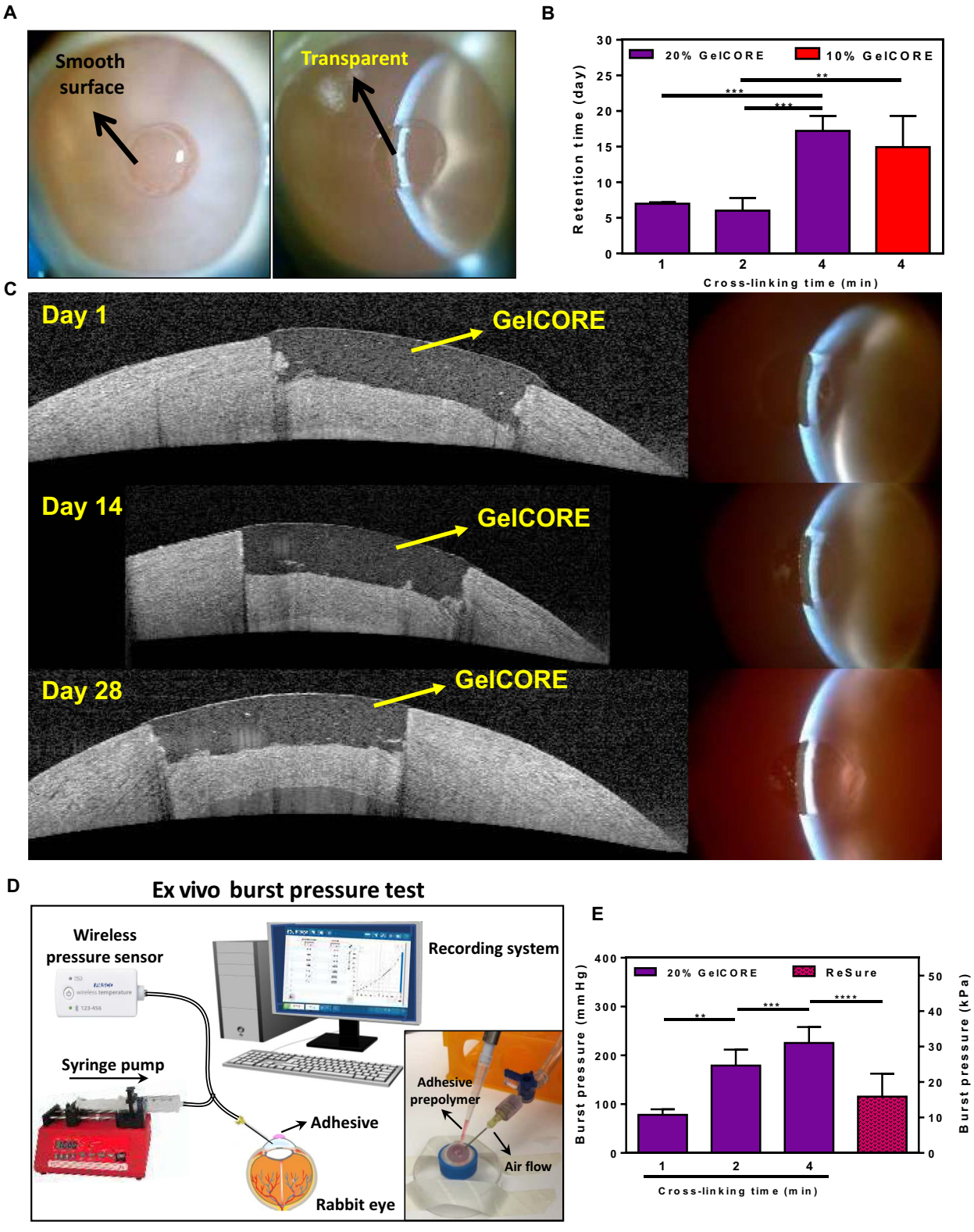

Fig. 3. Ex vivo application and adhesion properties of GelCORE adhesives. (**A**) Representative slit lamp photographs from rabbit eyes sealed by GelCORE bioadhesive, and (**B**) retention times of GelCORE bioadhesives, formed at various cross-linking times and prepolymer concentrations, on cornea tissues. (**C**) Representative optical coherence tomography images after ex vivo application of GelCORE adhesives to rabbit corneas at days 1, 14, and 28 after application. (**D**) Schematic of ex vivo burst pressure set up, including a syringe pump, a pressure sensor, and a recording system. (**E**) Average burst pressure of GelCORE adhesives formed by varying photocrosslinking time, compared to a commercially available ocular sealant, ReSure (control). Data are represented as means ± SD (***P* < 0.01, ****P* < 0.001, and *****P* < 0.0001; $n \geq 4$). [Photo credit: (A) Ahmad Kheirkhah, MEE, Harvard Medical School; (D) Ehsan Shirzaei Sani, UCLA]

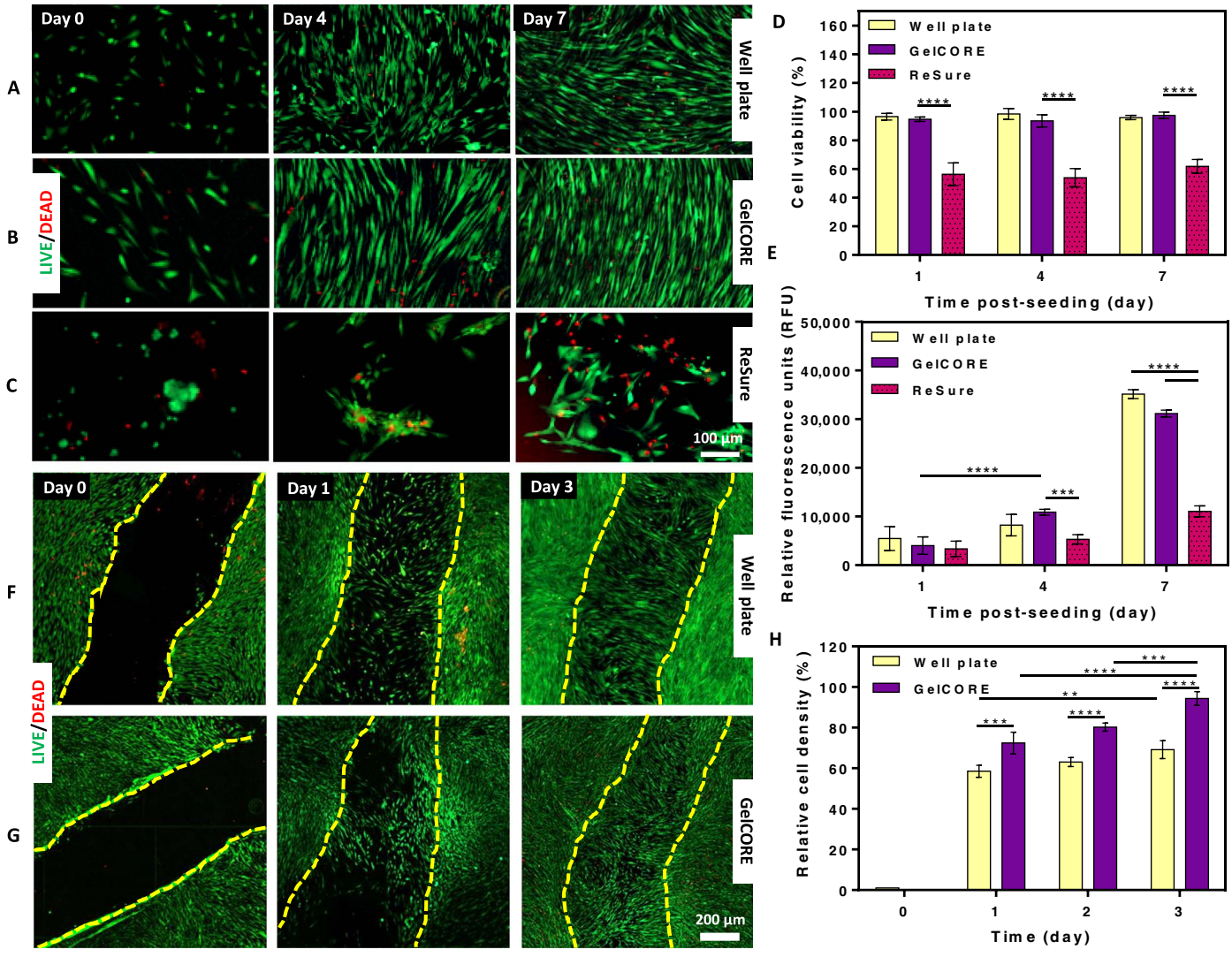

Fig. 4. In vitro cytocompatibility of GelCORE bioadhesives. Representative LIVE/DEAD images from corneal fibroblast cells seeded on (**A**) tissue culture well-plate, (**B**) GelCORE adhesives, and (**C**) ReSure sealant on days 1, 4, and 7 after seeding (scale bar, 100 µm). (**D**) Quantification of cell viability on GelCORE bioadhesives compared to tissue culture well plate and ReSure after 1, 4, and 7 days of culture. (**E**) Quantification of metabolic activity of corneal fibroblast cells seeded on control (tissue culture well plate), GelCORE hydrogels, and ReSure after 1, 4, and 7 days. Representative LIVE/DEAD images of corneal fibroblast cells grown on (**F**) tissue culture well plate and (**G**) GelCORE hydrogels based on a 2D scratch assay at 0, 1, and 3 days after scratching. (**H**) Quantification of relative cell densities migrated to the scratched area on GelCORE adhesives and control samples, at days 0, 1, 2, and 3. GelCORE hydrogels formed at 20% (w/v) final polymer concentration were used for 2D cell culture studies (photocrosslinking time, 4 min). Data are represented as means ± SD (**P < 0.01, ***P < 0.001, and ****P < 0.0001; $n \geq 3$).

cytotoxic and histotoxic effects on lung, arteries, and liver (*41*). In addition, it has been reported that BioGlue may cause serious nerve injury, mineralization, and coagulation necrosis (*9*), which dramatically reduces its possible application in ophthalmic surgeries (*9*). In contrast, our results indicated that GelCORE adhesive hydrogels prepared with visible light–initiated system are nontoxic to keratocytes. In addition, the adhesive hydrogel can support proliferation, adhesion and spreading, and metabolic activity of corneal cells in vitro. Therefore, GelCORE adhesive hydrogels maybe able to effectively enhance the healing process of corneal defects.

In vivo assessment of GelCORE bioadhesives in a rabbit stromal defect model

In our previous studies, we confirmed in vivo biocompatibility of UV and visible light cross-linked gelatin-based bioadhesives. This was done via subcutaneous implantation of disk-shaped hydrogels in rats (*32*) and in situ polymerization of gelatin-based sealants on incisions created on porcine lungs (*19*). In addition, we also confirmed in vivo biocompatibility of photocrosslinked gelatin hydrogel through direct injection into the myocardium and in situ polymerization (*29*). Our results showed that the hydrogels could degrade after 2 weeks without inducing significant inflammatory response while promoting tissue formation.

Herein, for the first time, we assessed the use of our engineered bioadhesives specifically designed for corneal sealing in a corneal injury model in New Zealand white rabbits. This was done by creating 50%-deep corneal defects in rabbit cornea (Fig. 5, A and B, and movies S2 and S3) to evaluate the biocompatibility and biointegration of the engineered GelCORE hydrogels for repair and sealing of corneal defects. After

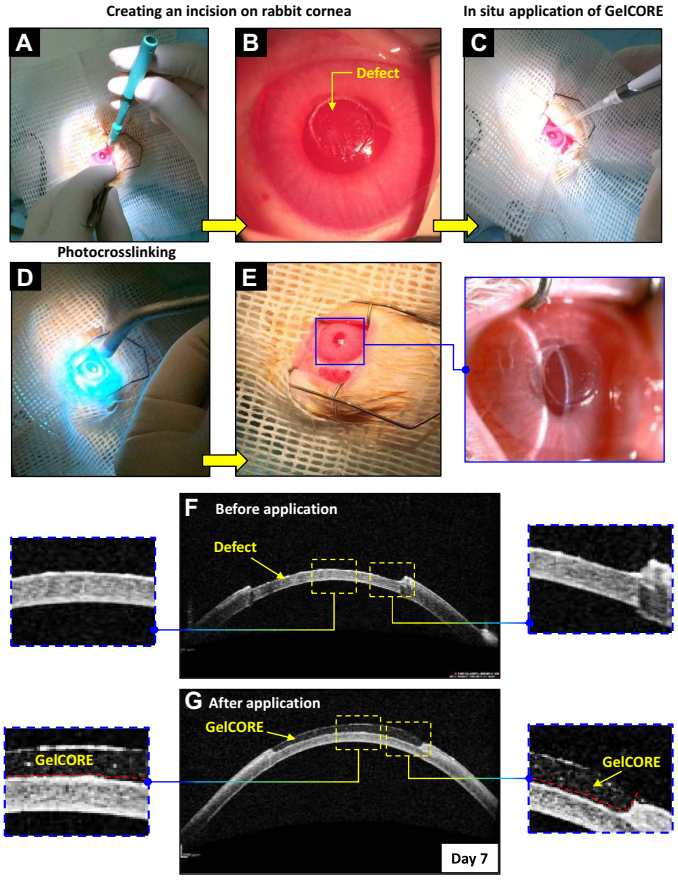

Fig. 5. In vivo application of GelCORE bioadhesives into corneal defects in rabbits. (**A** and **B**) Representative images for creating a 50% depth corneal stromal defect on rabbit eye. (**C**) In situ application of GelCORE prepolymer solution into corneal defect. (**D**) Photocrosslinking and (**E**) formation of a transparent GelCORE adhesive hydrogel on corneal stromal defect. AS-OCT images (**F**) before and (**G**) after treatment with GelCORE. Seven days after application, the bioadhesive still had a smooth surface. GelCORE hydrogels were prepared by using 20% (w/v) total polymer concentration and 4-min light exposure time. [Photo credit: (A to E) Amir Sheikhi, UCLA]

creating a half-thickness corneal stromal defect, a 20% (w/v) GelCORE bioadhesive precursor was applied into the defect site (Fig. 5C), followed by in situ polymerization via visible light for 4 min (Fig. 5D and movie S4) ($n \geq 4$). Immediately after photocrosslinking, there was a firm adhesion of the bioadhesive to the corneal defect (movies S5 and S6).

In addition, 1 day after surgery, the implanted bioadhesives were transparent, revealing a smooth surface. In addition, the surrounding cornea was transparent and noninflamed (Fig. 5E). AS-OCT also confirmed that the hydrogel was able to completely fill the defect and adhere to the stromal bed (Fig. 5, F and G). One week after surgery, the bioadhesive could be still observed on the defect site in the cornea and remained transparent (Fig. 5G).

In addition, as shown in Fig. 6A, the adhesive hydrogels remained transparent 1, 7, and 14 days after application. We also investigated whether there is migration of the epithelium over the adhesive hydrogel in the rabbit cornea. Cobalt blue slit lamp photographs with fluorescein staining showed progressive reduction of the size of corneal epithelial defect (Fig. 6B), implicating the migration of the epithelium over the bioadhesive (fluorescein stains epithelial defects in green). By day 14 after application, the corneal epithelial defect over the bioadhesive was completely healed (Fig. 6B).

Moreover, histological evaluation of cryo-sectioned tissues revealed the strong adhesion of GelCORE bioadhesive to the stromal tissue after application (Fig. 7B). In addition, the results showed growth of noninflammatory stromal tissue without any dominant deposition of a fibrous collagenous capsule after 14 days of application (Fig. 7D), which was similar to native cornea (Fig. 7A). Furthermore, histological assessment showed that the thickness of the corneal stromal layer for GelCORE-treated samples (582.2 ± 95.8 μm) was in the same range as that of the native rabbit cornea (554.9 ± 39.1 μm) (Fig. 7E). The stromal layer in untreated samples could not regenerate properly (Fig. 7C) and exhibited a thickness of 177.9 ± 39.3 μm (Fig. 7E). The thickness of the corneal epithelial layer was also evaluated histologically. Results revealed no statistically significant differences in the thickness of corneal epithelial layers in GelCORE treated, untreated, and native corneas (Fig. 7F). However, untreated samples showed a comparatively larger SD for thickness of the corneal epithelial layer as compared to native tissue

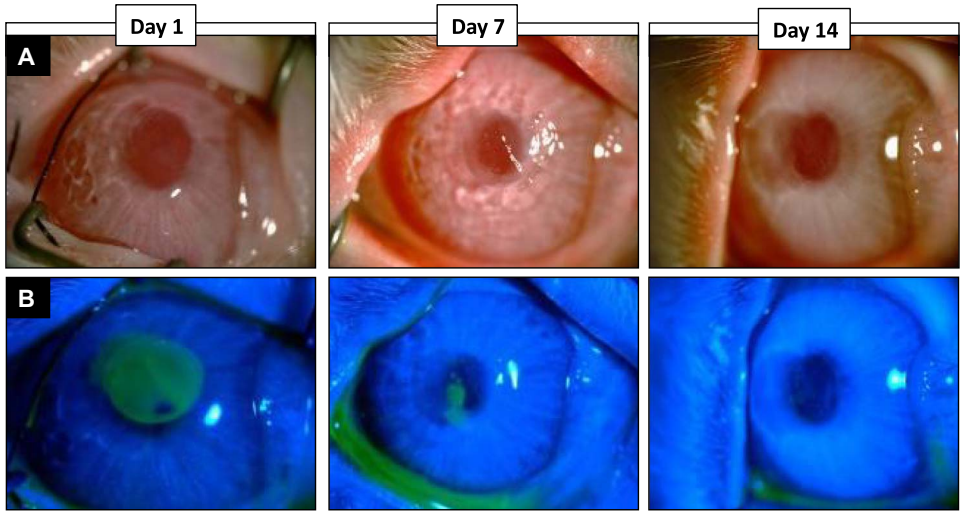

Fig. 6. Corneal re-epithelialization after in vivo application of the bioadhesive to corneal defects in rabbit cornea. (**A**) Representative slit lamp photographs and (**B**) cobalt blue with fluorescein staining after in vivo application of GelCORE adhesive to rabbit cornea at different time points. Progressive reduction in the size of corneal epithelial defect (green area in the central cornea) implicates epithelial migration over GelCORE. (Photo credit: Ahmad Kheirkhah, MEE, Harvard Medical School)

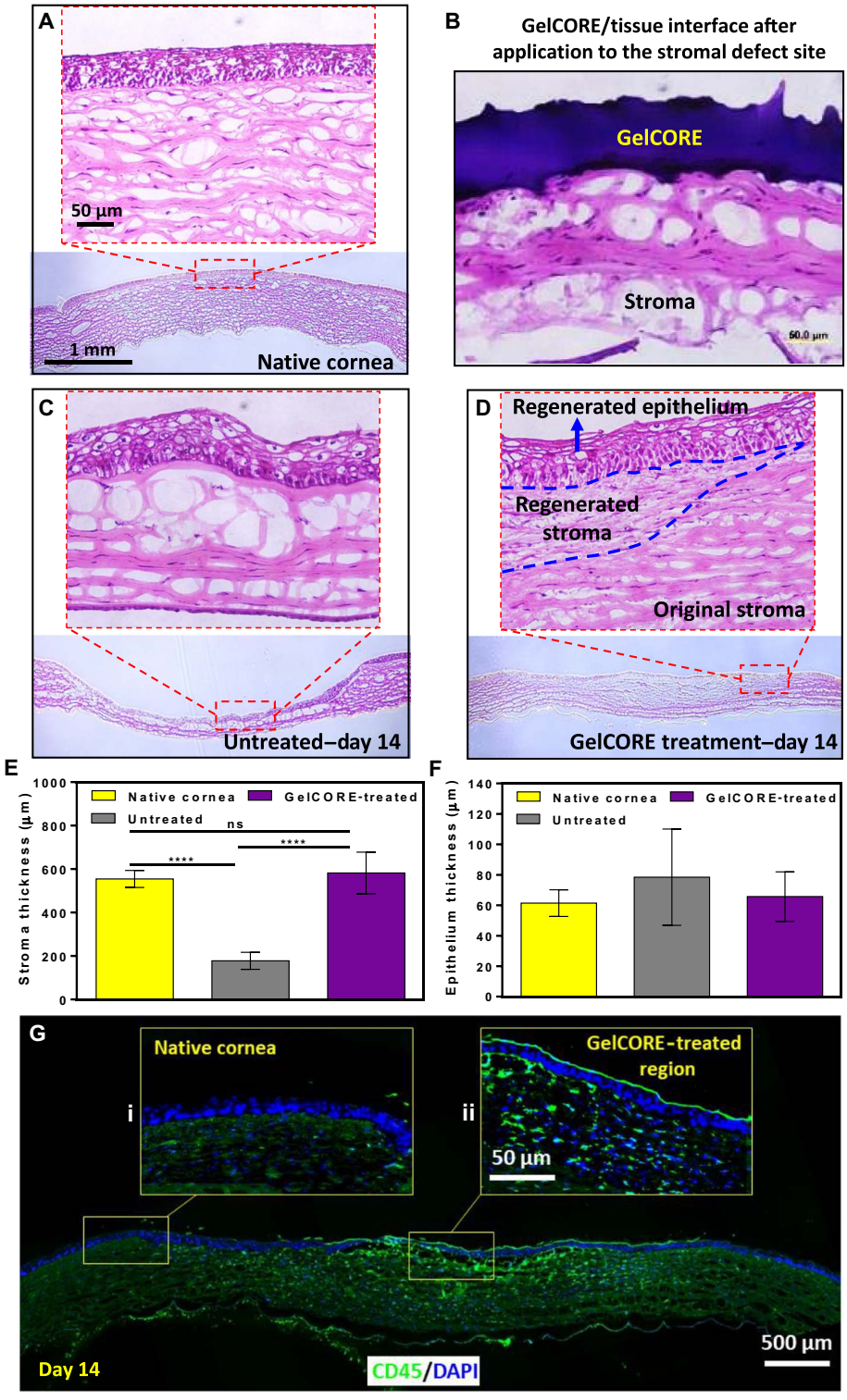

Fig. 7. Histological analysis after application of GelCORE bioadhesive in a rabbit corneal stromal defect model. Representative hematoxylin and eosin histopathology images from (**A**) native rabbit corneas (without defect) and (**B**) rabbit cornea after application of GelCORE in a 50% depth stromal defect. Histological images for (**C**) untreated stromal defect (without bioadhesive) and (**D**) the defect treated with bioadhesive at day 14 after surgery (scale bars, 50 µm and 1 mm). (**E**) Thickness of stromal layer for the native cornea, GelCORE-treated, and untreated eyes at day 14 after surgery obtained from histological images. (**F**) Thickness of epithelial layer for native cornea and GelCORE-treated and untreated eyes at day 14 after surgery obtained from histological images. (**G**) Representative fluorescent immunohistochemical images (DAPI and CD45 marker) (i) from the area without defect and (ii) from corneal stromal defect treated with GelCORE bioadhesive at day 14 after surgery. GelCORE hydrogels were prepared at 20% (w/v) total polymer concentration and 4-min light exposure time. Data are represented as means ± SD (****$P < 0.0001$; $n \geq 3$).

which indicates heterogenous re-epithelialization of untreated samples (Fig. 7F).

The thickness of the corneal epithelial layer was also evaluated histologically. Results revealed no statistically significant differences in the thickness of corneal epithelial layers in GelCORE-treated, untreated, and native corneas (Fig. 7F). However, untreated samples showed a larger SD for thickness of the corneal epithelial layer as compared to native tissue, which indicates heterogeneous re-epithelialization of untreated samples (Fig. 7F). The immunostaining results (DAPI staining) also indicated homogenous re-epithelialization in GelCORE treated group (Fig. 7Gii) after 14 days, similar to native cornea (Fig. 7Gi). Moreover, leukocyte infiltration was detected by expression of CD45 maker in the GelCORE-treated corneas, showing normal inflammatory responses during the regeneration process (Fig. 7Gii) (*43*). In addition, an autologous tissue regeneration was observed for the defects treated with GelCORE bioadhesive after 14 days of application (Fig. 7Gii). The cell nuclei within the new tissue showed the similarities between regenerated tissue and native tissue (Fig. 7G).

DISCUSSION

Conventional standards of care for corneal stromal defects have significant drawbacks including poor biomechanical, optical, or adhesive properties, as well as lack of biocompatibility and regenerative capability. To overcome these limitations, in this study, we developed a biocompatible and adhesive hydrogel for corneal tissue sealing and repair. In our system, gelatin is chemically functionalized with methacryloyl groups to form a visible light activated GelCORE bioadhesive. Our results show that physical properties and adhesion strength of GelCORE bioadhesives can be tuned by changing GelCORE concentration and light exposure time. In vitro cell studies show that engineered hydrogels are cytocompatible with corneal cells and promote cell integration after application. Furthermore, in vivo experiments show that GelCORE can effectively seal corneal defects and promote re-epithelialization. Other researchers have also aimed to develop tissue-engineered transplants for the treatment of corneal epithelial defects and stromal ulcers to reduce the dependence on donor corneas. However, the majority of these methods are based on prefabricated membranes (*13*) or patches (*33*), which typically require surgical equipment and skills. In addition, most of these prefabricated transplants are "passive" cell-based approaches, which are potentially associated with high cell loss during implantation and immunogenicity (*44*, *45*). In contrast, our approach uses a biocompatible adhesive for sutureless and cell-free sealing and treatment of corneal stromal defects without requiring advanced surgical procedures. In addition, different tissue adhesives, including fibrin-based (i.e., fibrin glue, Tisseel) and PEG-based (i.e., ReSure) bioadhesives, have also been tested for ophthalmic applications. The major drawback of these adhesives is that they lack high adhesion to wet corneal tissue, nor do they have long retention (*9*). Fibrin-based adhesives may also have the risk of transmitted diseases from pooled and single blood donors (*46*). PEG-based bioadhesives also suffer from similar limitations, including uncontrolled cross-linking, which are impractical in a clinical setting, and they lack the required mechanical properties that would efficiently promote regeneration (*9*).

Last, an important feature of the GelCORE biomaterial is its ability to permit normal regenerative responses while it fills in corneal stromal defects of different size and geometry. This can lead to corneal tissue regeneration, encourages faster recovery of patients, reduces the need for future visual rehabilitative measures, and, in some cases, circumvent the need for corneal transplantation. Overall, our results showed that the bioengineered GelCORE adhesive has many advantages highlighted throughout this study, making it a promising substance for use in corneal repair.

MATERIALS AND METHODS

Fabrication of GelCORE bioadhesive hydrogels

GelCORE prepolymer was synthesized on the basis of previously published protocol (*19*). Briefly, 10 g of porcine gelatin (Sigma-Aldrich) was dissolved in 100 ml of DPBS and heated at 60°C for 1 hour. Next, 8 ml of methacrylic anhydride (Sigma-Aldrich) was added dropwise to gelatin solution under continuous stirring at 50°C for 3 hours. The solution was then diluted with DPBS and dialyzed against deionized water at 50°C for 5 days. The resulting solution was then filtered and lyophilized for 3 days. The photoinitiator solution was prepared by dissolving TEA [1.875% (w/v)], VC [1.25% (w/v)], and Eosin Y disodium salt (0.5 mM) in distilled water at 37°C. GelCORE precursor solutions were prepared by dissolving varying concentrations of GelCORE [5, 10, and 20% (w/v)] in the photoinitiator solution. The bioadhesive prepolymer solution was then vortexed at 37°C, and immediately, 70 μl of the precursor solution was pipetted into polydimethylsiloxane cylindrical molds (diameter, 6 mm; height, 2.5 mm) for compression testing, or rectangular molds (14 mm by 5 mm by 1 mm) for tensile testing. The solution was then photocrosslinked with visible light (450 to 550 nm) for 1, 2, and 4 min, using an LS1000 Focal Seal Xenon Light Source (100 mW/cm^2, Genzyme).

^{1}H NMR analysis of GelCORE bioadhesives

^{1}H NMR analysis was performed to measure degree of cross-linking of GelCORE bioadhesive hydrogels as described elsewhere (*32*). Briefly, GelCORE adhesives were prepared in cylindrical molds and lyophilized as described earlier. Then, both GelCORE adhesives and prepolymer were partially dissolved in DMSO-d6. ^{1}H NMR spectra were obtained from GelCORE bioadhesive hydrogels at different cross-linking times and prepolymer solutions using a Varian Inova-500 NMR spectrometer. The peaks for the hydrogen atoms in methacryloyl (methacrylate and methacrylamide) groups were identified at δ = 5.3 and 5.7 ppm. Next, the area under these peaks was integrated for all the samples. At different light exposure times, the changes in the integrated area with respect to prepolymer solution were reported as degrees of cross-linking of bioadhesive hydrogels. This area was calculated using the following equation

$$\text{Decay of methacryloyl groups } (\%) = \frac{A_b - A_a}{A_b} \times 100 \qquad (1)$$

where A_b and A_a show the integrated areas of methacryloyl groups before and after photocrosslinking, respectively.

Mechanical characterization of the GelCORE bioadhesives

Hydrogels were prepared as described above. The precise dimensions of the fabricated bioadhesives were obtained using a digital caliper. Mechanical testing (tensile and compression) was conducted using an Instron 5542 mechanical tester. For tensile tests, rectangular hydrogels were fixed between double-sided tapes fastened to the Instron's tension grips. Samples were stretched at a rate of 1 mm/min until rupture. The load (in newtons) and tensile strain (in millimeters) values were recorded using the accompanying Bluehill 3 software. Elastic moduli of

the fabricated bioadhesives were obtained by measuring the slope of the stress-strain curves (0.1 to 0.3 mm/mm strain). The UTS was obtained from the point of failure. For compressive experiments, cylindrical bioadhesives were placed in the Instron's compressive plates in a DPBS bath. The compression test was conducted at a rate of 1 mm/min up to a max strain of 70%. Similarly, the values for compressive strain (in millimeters) and load (in newtons) were recorded using the Bluehill 3 software. The compressive moduli were calculated from the slope of the linear region (0.1 to 0.2 mm/mm strain) on the stress (in kilopascals) versus strain (millimeter per millimeter) curves ($n \geq 3$).

In vitro adhesion tests

Burst pressure test

Sealing capability of engineered bioadhesives and commercially available sealants, CoSEAL (Baxter, Deerfield, IL, USA) and Evicel (Ethicon, Somerville, NJ, USA), were measured according to a modified ASTM standard, F2392-04, for burst pressure, as described previously (*47*). Briefly, porcine intestine was fixed in the middle of two stainless steel annuli, using a custom-made burst pressure apparatus in which the upper annuli contained a 10-mm-diameter hole. Using an 18-gauge syringe needle, a 2-mm-diameter hole was created in the intestine tissue. Next, 30 μl of prepolymer solution was pipetted on the defect area and quickly cross-linked by visible light. Next, the air was applied into the system, and the maximum burst pressure was recorded by using a wireless sensor (Pasco) ($n \geq 3$).

Lap shear test

Shear strength of GelCORE bioadhesive, as well as Evicel, and CoSEAL were measured using a modified lap shear test based on ASTM standard, F2255-05 according to previously published protocol (*47*). As a replacement for the substrate, two pieces of glass slides (10 mm by 50 mm) were coated with a 20% (w/v) gelatin solution at 37°C and were dried at room temperature. Next, 10 μl of precursor solution was pipetted and photocrosslinked between two pieces of glass slides. The shear strengths of the samples were then tested using an Instron mechanical tester, as described previously. Tensile stress was then applied (1 mm/min), and the shear strengths of the bioadhesives were measured at the detachment point ($n \geq 3$).

Wound closure test

Wound closure capability of GelCORE bioadhesives, as well as Evicel and CoSEAL were measured using a modified ASTM standard test, F2458-05 (*48*). Porcine skin, purchased from a local butcher shop, was cut into small pieces (1 cm by 2 cm), and the excess fat was removed. The porcine skins were kept hydrated in DPBS before testing and then fixed onto two pieces of glass slides (20 mm by 60 mm) by superglue. The space between glass slides was adjusted to 10 mm by using the tissue. An incision was made to simulate a wound using a straight edge razor. One hundred milliliters of polymer solution was administered onto the wound site and cross-linked via exposure to visible light. The ultimate adhesive strength of bioadhesives was measured at the detachment point using an Instron mechanical tester. Tensile loading was conducted at strain rate of 1 mm/min using the Instron mechanical tester as described above ($n \geq 5$).

In vitro measurement of water content of the adhesive hydrogels

Adhesive hydrogels were prepared as described before. The wet weights of the fresh samples were then measured. Samples were subsequently immersed in DPBS for 48 hours. The weights of each hydrogel were recorded at varying time points. The water content was then calculated using Eq. 2, where W_S is swollen weight of the bioadhesive and W_D is the initial weight before swelling ($n \geq 4$)

$$\text{Water content} = \frac{W_S - W_D}{W_D} \times 100 \quad (2)$$

In vitro enzymatic degradation of the adhesive hydrogels

The in vitro degradation of bioadhesives was examined as described previously (*47*). Disc-shaped GelCORE samples (d = 6 mm; h = 3 mm) were formed as described before. Next, the initial weights of the samples were measured, and the samples were incubated in different concentrations (0, 2.5, 5, and 40 μg/ml) of collagenase type II (Thermo Fisher Scientific) in DPBS for 1, 2, 3, 4, 7, and 10 days. At each time point, the final weights of the samples were measured. The degradation percentage of each sample was calculated based on the weight loss over time.

In vitro cell studies

Cell lines

Corneal fibroblast cells [American Type Culture Collection (ATCC)] were cultured at 37°C and 5% CO_2 in Dulbecco's modified Eagle's medium (DMEM): Nutrient Mixture F-12 (DMEM/F12) (Sigma-Aldrich) containing 10% (v/v) fetal bovine serum, 1% (v/v) antibiotic/antimycotics (Sigma-Aldrich), and 1% (v/v) L-glutamine (Sigma-Aldrich). Cells were maintained in flasks (tissue culture treated) and passaged when reached to 70% confluency.

2D cell seeding on GelCORE bioadhesives

Hydrogel prepolymer solution was prepared as previously described. Seven microliters of precursor solution was then pipetted between a 3-(trimethoxysilyl) propyl methacrylate (TMSPMA; Sigma-Aldrich)–coated glass slide and a petri dish separated with a 300-μm spacer. The prepolymer solutions were then photocrosslinked for 4 min via visible light. Next, 40 μl of corneal fibroblast cell solution (2×10^6 cells/ml) was seeded on each sample. After 45-min incubation, 360 μl of cell culture media was added to each sample, and they were maintained at 37°C and 5% CO_2 for 5 days. In addition, cells at the same density were also seeded inside 24-well tissue culture plates. As the commercial control, the tissue culture well plates were coated with ReSure sealant, and the same cell density (40 μl, 2×10^6 cells/ml) was seeded in each well.

2D cell scratch test

Hydrogel prepolymer solution was prepared as previously described. Forty microliters of precursor solution was then pipetted between a TMSPMA-coated glass slide and a petri dish separated with a 300-μm spacer. Hydrogels were then photocrosslinked for 4 min via exposure to visible light. Corneal fibroblast cells (2×10^6 cells/ml) were then seeded on the hydrogels and maintained at 37°C and 5% CO_2. After 2 days, the cell layer on the surface of the hydrogels was scratched using a 1-ml pipette tips. The cells were stained at day 0, 1, 2 and 3 after creating scratch. Polystyrene 24-well plates were used as control.

Determination of cell proliferation

PrestoBlue assay (Thermo Fisher Scientific) was used for determination of cell proliferation using the instruction provided by the manufacturer. Briefly, cells seeded on the adhesives were stained with a solution containing 10% (v/v) PrestoBlue dye in media. Then, the samples were incubated for 1 hour at 37°C in the PrestoBlue/medium solution before measuring fluorescence. Fluorescence intensity of the stained solution was then measured at 535- to 560-nm excitation and 590- to 615-nm emission wavelength on days 1, 4, and 7 of culture.

Determination of cell viability

The viability of corneal fibroblast cells was obtained using a calcein acetoxymethyl (calcein AM) and ethidium homodimer-1 LIVE/DEAD assay from Invitrogen based on the instruction provided by the manufacturer. Briefly, calcein AM (0.5 μl/ml) and ethidium homodimer-1 (2 μl/ml) were diluted in DPBS to form the staining solution. Cell medium was removed from wells containing scaffolds, and 100 μl of staining solution was added. Cell-seeded scaffolds were then incubated for 15 min at 37°C, in the dark. Live (green stain) and dead (red stain) cells were imaged using an inverted fluorescent microscope from ZEISS (Axio Observer Z1). Last, the cell viability was quantified by dividing the number of the live cells by total number of cells, using ImageJ software.

Determination of cell adhesion and spreading

Cell spreading in 2D cultures was visualized by F-actin microfilaments and cell nuclei fluorescent staining, as described previously (*47*). Briefly, cell seeded hydrogels were washed with DPBS (three times) and then fixed with 4% (v/v) paraformaldehyde solution (Sigma-Aldrich) for 20 min. After fixation, the samples were washed again three times with DPBS. Fixed samples were permeabilized in 0.1% (w/v) Triton X-100 (Sigma-Aldrich) in DPBS for 20 min. The samples were then triple-washed with DPBS, and cell actin filament was stained via Alexa Fluor 488–labeled phalloidin [1.25% (v/v) in 0.1% bovine serum albumin, Invitrogen] for 45 min, followed by another triple wash with DPBS. Last, cell nuclei were stained with DAPI (1 μl/ml; Sigma-Aldrich) in DPBS for 5 min, followed by a final wash with DPBS. Immediate microscopy image acquisition was performed using an Axio Observer Z1 inverted microscope.

Rabbit corneal surgeries

Surgical procedures

For in vivo experiments, 8- to 12-week-old male New Zealand white rabbits were purchased from the Jackson Laboratories (Bar Harbor, ME). Survival surgeries in rabbits were performed under aseptic conditions. To induce corneal injury, a lamellar (partial thickness) keratectomy was performed in rabbit eyes. For this, after general anesthesia using intramuscular injection of ketamine (30 to 50 mg/kg) and xylazine (5 to 10 mg/kg) and topical anesthesia proparacaine 0.5% ophthalmic solution, a 3-mm biopsy punch was used to make a partial trephination (cut) in the central cornea of the right eye to a depth of approximately 50%. Then, a surgical knife was used to perform a lamellar keratectomy at the same depth. The bioadhesives were then applied and photopolymerized as described before [20% (w/v), 4-min visible light exposure time]. Following the surgical procedures, the rabbits were kept warm by placing them on a heating pad until recovery from the anesthesia. All the rabbits received buprenorphine (0.01 to 0.5 mg/kg) by subcutaneous injection every 12 hours for 48 hours. The rabbit eyes were then evaluated using slit lamp biomicroscopy and AS-OCT at 1 and 2 weeks after surgery. These tests were also performed under general anesthesia as described before. At the end of the study, the rabbits were euthanized, and the eyes were explanted for histologic analysis (after 2 weeks).

Slit lamp biomicroscopy

Slit lamp biomicroscopy was performed under general anesthesia using a Topcon system. Slit lamp photographs were also taken at the time of examination. With a ×16 magnification, using slit and broad beams, transparency of the bioadhesive and the surrounding cornea was evaluated. To assess the migration of corneal epithelium over the adhesive, cobalt blue slit lamp photography with fluorescein staining was performed.

Anterior segment optical coherence tomography

AS-OCT was performed under general anesthesia at days 0, 7, and 14 after surgery. AS-OCT is a high-resolution cross-sectional and noncontact imaging system. A spectral-domain AS-OCT (Spectralis, Heidelberg Engineering, Germany), with an axial resolution of 3.9 to 7 μm, was used for imaging.

Histological analysis

After explantation of the rabbit corneas, the samples were fixed in 4% (v/v) paraformaldehyde overnight. Next, they were embedded in optimal cutting temperature compound and quickly frozen in liquid nitrogen. Using a Leica Biosystems CM3050 S Research Cryostat, the samples were then sectioned (6 μm) and fixed on positively charged glass slides. For the staining, a hematoxylin and eosin kit (Sigma-Aldrich) was used according to the manufacturer's instructions. For immunostaining, anti-CD45 antibody (ab10558) (Abcam) and Alexa Fluor 488–conjugated (Invitrogen) were used as primary and secondary antibodies according to manufacturer's protocol. Next, the slides were mounted with DPX mountant medium (Sigma-Aldrich) and visualized on an AxioObserver Z1 inverted microscope.

Statistical analysis

For each experiment, at least three samples were tested, and data were presented as means ± SD (*$P < 0.05$, **$P < 0.01$, ***$P < 0.001$, and ****$P < 0.0001$). One-way or two-way analysis of variance (ANOVA) *t* test was performed followed by Tukey's test for statistical analysis (GraphPad Prism 6.0, GraphPad Software).

SUPPLEMENTARY MATERIALS

Supplementary material for this article is available at http://advances.sciencemag.org/cgi/content/full/5/3/eaav1281/DC1

Fig. S1. ^{1}H NMR spectra of GelCORE prepolymer and GelCORE bioadhesives.
Fig. S2. Quantification of degree of cross-linking for GelCORE hydrogels.
Fig. S3. UTS of GelCORE hydrogels.
Fig. S4. Representative actin/DAPI images for corneal fibroblast cells seeded on GelCORE hydrogels.
Movie S1. Ex vivo adhesion of GelCORE bioadhesives on rabbit eyes.
Movie S2. Creating corneal defect in rabbit cornea using a biopsy punch.
Movie S3. Creating corneal defect in rabbit cornea using a surgical knife.
Movie S4. Photocrosslinking of the GelCORE bioadhesive with visible light.
Movie S5. Firm adhesion of the bioadhesive to the corneal defect.
Movie S6. Firm adhesion of the bioadhesive to the corneal defect.

REFERENCES AND NOTES

1. M. M. Islam, O. Buznyk, J. C. Reddy, N. Pasyechnikova, E. I. Alarcon, S. Hayes, P. Lewis, P. Fagerholm, C. He, S. Iakymenko, W. Liu, K. M. Meek, V. S. Sangwan, M. Griffith, Biomaterials-enabled cornea regeneration in patients at high risk for rejection of donor tissue transplantation. *NPJ Regen. Med.* **3**, 2 (2018).
2. P. Gain, R. Jullienne, Z. He, M. Aldossary, S. Acquart, F. Cognasse, G. Thuret, Global survey of corneal transplantation and eye banking. *JAMA Ophthalmol.* **134**, 167–173 (2016).
3. A. V. Ljubimov, M. Saghizadeh, Progress in corneal wound healing. *Prog. Retin. Eye Res.* **49**, 17–45 (2015).
4. G. Ciapetti, S. Stea, E. Cenni, A. Sudanese, D. Marraro, A. Toni, A. Pizzoferrato, Cytotoxicity testing of cyanoacrylates using direct contact assay on cell cultures. *Biomaterials* **15**, 63–67 (1994).
5. C. Matossian, S. Makari, R. Potvin, Cataract surgery and methods of wound closure: A review. *Clin. Ophthalmol.* **9**, 921–928 (2015).
6. K. Nishida, M. Yamato, Y. Hayashida, K. Watanabe, K. Yamamoto, E. Adachi, S. Nagai, A. Kikuchi, N. Maeda, H. Watanabe, T. Okano, Y. Tano, Corneal reconstruction with tissue-engineered cell sheets composed of autologous oral mucosal epithelium. *N. Eng. J. Med.* **351**, 1187–1196 (2004).
7. B. Kharod-Dholakia, J. B. Randleman, J. G. Bromley, R. D. Stulting, Prevention and treatment of corneal graft rejection: current practice patterns of the Cornea Society (2011). *Cornea* **34**, 609–614 (2015).

8. Z. Chen, J. You, X. Liu, S. Cooper, C. Hodge, G. Sutton, J. M. Crook, G. G. Wallace, Biomaterials for corneal bioengineering. *Biomed. Mater.* **13**, 032002 (2018).
9. H. C. Park, R. Champakalakshmi, P. P. Panengad, M. Raghunath, J. S. Mehta, Tissue adhesives in ocular surgery. *Expert Rev. Ophthalmol.* **6**, 631–655 (2011).
10. H. S. Uy, K. R. Kenyon, Surgical outcomes after application of a liquid adhesive ocular bandage to clear corneal incisions during cataract surgery. *J. Cataract Refract. Surg.* **39**, 1668–1674 (2013).
11. L. Li, C. Lu, L. Wang, M. Chen, J. White, X. Hao, K. M. McLean, H. Chen, T. C. Hughes, Gelatin-based photocurable hydrogels for corneal wound repair. *ACS Appl. Mater. Interfaces* **10**, 13283–13292 (2018).
12. D. M. Maurice, The structure and transparency of the cornea. *J. Physiol.* **136**, 263–286 (1957).
13. J. J. Chae, W. M. Ambrose, F. A. Espinoza, D. G. Mulreany, S. Ng, T. Takezawa, M. M. Trexler, O. D. Schein, R. S. Chuck, J. H. Elisseeff, Regeneration of corneal epithelium utilizing a collagen vitrigel membrane in rabbit models for corneal stromal wound and limbal stem cell deficiency. *Acta Ophthalmol.* **93**, e57–e66 (2015).
14. X. Calderón-Colón, Z. Xia, J. L. Breidenich, D. G. Mulreany, Q. Guo, O. M. Uy, J. E. Tiffany, D. E. Freund, R. L. McCally, O. D. Schein, J. H. Elisseeff, M. M. Trexler, Structure and properties of collagen vitrigel membranes for ocular repair and regeneration applications. *Biomaterials* **33**, 8286–8295 (2012).
15. M. Banitt, J. B. Malta, H. K. Soong, D. C. Musch, S. I. Mian, Wound integrity of clear corneal incisions closed with fibrin and N-butyl-2-cyanoacrylate adhesives. *Curr. Eye Res.* **34**, 706–710 (2009).
16. J. Rose, S. Pacelli, A. J. El Haj, H. S. Dua, A. Hopkinson, L. J. White, F. R. A. J. Rose, Gelatin-based materials in ocular tissue engineering. *Materials* **7**, 3106–3135 (2014).
17. D. N. Mishra, R. M. Gilhotra, Design and characterization of bioadhesive in-situ gelling ocular inserts of gatifloxacin sesquihydrate. *DARU J. Pharm. Sci.* **16**, 1–8 (2008).
18. T. Gratieri, G. M. Gelfuso, E. M. Rocha, V. H. Sarmento, O. de Freitas, R. F. Lopez, A poloxamer/chitosan in situ forming gel with prolonged retention time for ocular delivery. *Eur. J. Pharm. Biopharm.* **75**, 186–193 (2010).
19. A. Assmann, A. Vegh, M. Ghasemi-Rad, S. Bagherifard, G. Cheng, E. S. Sani, G. U. Ruiz-Esparza, I. Noshadi, A. D. Lassaletta, S. Gangadharan, A. Tamayol, A. Khademhosseini, N. Annabi, A highly adhesive and naturally derived sealant. *Biomaterials* **140**, 115–127 (2017).
20. C. Kielbassa, L. Roza, B. Epe, Wavelength dependence of oxidative DNA damage induced by UV and visible light. *Carcinogenesis* **18**, 811–816 (1997).
21. F. Behar-Cohen, G. Baillet, T. de Ayguavives, P. Ortega Garcia, J. Krutmann, P. Peña-García, C. Reme, J. S. Wolffsohn, Ultraviolet damage to the eye revisited: Eye-sun protection factor (E-SPF®), a new ultraviolet protection label for eyewear. *Clin. Ophthalmol.* **8**, 87–104 (2014).
22. H.-Y. Youn, D. J. McCanna, J. G. Sivak, L. W. Jones, In vitro ultraviolet–induced damage in human corneal, lens, and retinal pigment epithelial cells. *Mol. Vis.* **17**, 237–246 (2011).
23. K. Ramasamy, S. Mohana, B. Agilan, G. Kanimozhi, G. Srithar, M. Ganesan, R. Beualah Mary, N. R. Prasad, Ultraviolet radiation-induced carcinogenesis: Mechanisms and experimental models. *J. Cancer Res. Ther.* **8**, 4–19 (2017).
24. J. P. G. Bergmanson, P. G. Söderberg, The significance of ultraviolet radiation for eye diseases. A review with comments on the efficacy of UV-blocking contact lenses. *Ophthalmic Physiol. Opt.* **15**, 83–91 (1995).
25. F. C. Delori, R. H. Webb, D. H. Sliney, Maximum permissible exposures for ocular safety (ANSI 2000), with emphasis on ophthalmic devices. *J. Opt. Soc. Am. A* **24**, 1250–1265 (2007).
26. S. J. Bryant, C. R. Nuttelman, K. S. Anseth, Cytocompatibility of UV and visible light photoinitiating systems on cultured NIH/3T3 fibroblasts in vitro. *J. Biomater. Sci. Polym. Ed.* **11**, 439–457 (2000).
27. H. Lin, A. W. Cheng, P. G. Alexander, A. M. Beck, R. S. Tuan, Cartilage tissue engineering application of injectable gelatin hydrogel with in situ visible-light-activated gelation capability in both air and aqueous solution. *Tissue Eng. Part. A.* **20**, 2402–2411 (2014).
28. M. J. R. Soucy, E. Shirzaei Sani, R. Portillo Lara, D. Diaz, F. Dias, A. S. Weiss, A. N. Koppes, R. A. Koppes, N. Annabi, Photocrosslinkable gelatin/tropoelastin hydrogel adhesives for peripheral nerve repair. *Tissue Eng. Part A* **0**, 1393–1405 (2018).
29. I. Noshadi, S. Hong, K. E. Sullivan, E. Shirzaei Sani, R. Portillo-Lara, A. Tamayol, S. Ryon Shin, A. E. Gao, W. L. Stoppel, L. D. Black III, A. Khademhosseini, N. Annabi, In vitro and in vivo analysis of visible light crosslinkable gelatin methacryloyl (GelMA) hydrogels. *Biomater. Sci.* **5**, 2093–2105 (2017).
30. N. Annabi, K. Yue, A. Tamayol, A. Khademhosseini, A. Khademhosseini, Elastic sealants for surgical applications. *Eur. J. Pharm. Biopharm.* **95**, 27–39 (2015).
31. C. Bahney, T. J. Lujan, C. W. Hsu, M. Bottlang, J. L. West, B. Johnstone, Visible light photoinitiation of mesenchymal stem cell-laden bioresponsive hydrogels. *Eur. Cell. Mater.* **22**, 43–55 (2011).
32. N. Annabi, D. Rana, E. Shirzaei Sani, R. Portillo-Lara, J. L. Gifford, M. M. Fares, S. M. Mithieux, A. S. Weiss, Engineering a sprayable and elastic hydrogel adhesive with antimicrobial properties for wound healing. *Biomaterials* **139**, 229–243 (2017).
33. M. Rizwan, G. S. L. Peh, H.-P. Ang, N. C. Lwin, K. Adnan, J. S. Mehta, W. S. Tan, E. K. F. Yim, Sequentially-crosslinked bioactive hydrogels as nano-patterned substrates with customizable stiffness and degradation for corneal tissue engineering applications. *Biomaterials* **120**, 139–154 (2017).
34. M. Pircher, E. Götzinger, R. Leitgeb, A. F. Fercher, C. K. Hitzenberger, Measurement and imaging of water concentration in human cornea with differential absorption optical coherence tomography. *Opt. Express* **11**, 2190–2197 (2003).
35. D.-A. Wang, S. Varghese, B. Sharma, I. Strehin, S. Fermanian, J. Gorham, D. Howard Fairbrother, B. Cascio, J. H. Elisseeff, Multifunctional chondroitin sulphate for cartilage tissue-biomaterial integration. *Nat. Mater.* **6**, 385–392 (2007).
36. A. Lauto, D. Mawad, L. J. R. Foster, Adhesive biomaterials for tissue reconstruction. *J. Chem. Technol. Biotechnol.* **83**, 464–472 (2008).
37. R. P. Pawar, A. E. Jadhav, S. B. Tathe, B. C. Khade, A. J. Domb, in *Biodegradable Polymers in Clinical Use and Clinical Development*, A. J. Domb, N. Kumar, A. Ezra, Ed. (John Wiley & Sons Inc., 2011), pp. 417–450.
38. P. K. Campbell, S. L. Bennett, A. Driscoll, A. S. Sawhney, Evaluation of Absorbable Surgical Sealants: In vitro Testing (Covidien, 2005).
39. W. D. Spotnitz, Fibrin sealant: The only approved hemostat, sealant, and adhesive; a laboratory and clinical perspective. *ISRN Surg.* **2014**, 203943 (2014).
40. W.-L. Chen, C. T. Lin, C. Y. Hsieh, I. H. Tu, W. Y. Chen, F. R. Hu, Comparison of the bacteriostatic effects, corneal cytotoxicity, and the ability to seal corneal incisions among three different tissue adhesives. *Cornea* **26**, 1228–1234 (2007).
41. W. Fürst, A. Banerjee, Release of glutaraldehyde from an albumin-glutaraldehyde tissue adhesive causes significant in vitro and in vivo toxicity. *Ann. Thorac. Surg.* **79**, 1522–1528 (2005).
42. D. Hee Park, S. Bum Kim, K.-D. Ahn, E. Yong Kim, Y. Jun Kim, D. Keun Han, In vitro degradation and cytotoxicity of alkyl 2-cyanoacrylate polymers for application to tissue adhesives. *J. Appl. Polym. Sci.* **89**, 3272–3278 (2003).
43. Y. Ma, Y. Xu, Z. Xiao, W. Yang, C. Zhang, E. Song, Y. Du, L. Li, Reconstruction of chemically burned rat corneal surface by bone marrow–derived human mesenchymal Stem Cells. *Stem Cells* **24**, 315–321 (2006).
44. S. Kelaini, A. Cochrane, A. Margariti, Direct reprogramming of adult cells: Avoiding the pluripotent state. *Stem Cells Cloning* **7**, 19–29 (2014).
45. S. Murugesan, J. Xie, R. J. Linhardt, Immobilization of heparin: Approaches and applications. *Curr. Top. Med. Chem.* **8**, 80–100 (2008).
46. A. Panda, S. Kumar, A. Kumar, R. Bansal, S. Bhartiya, Fibrin glue in ophthalmology. *Indian J. Ophthalmol.* **57**, 371–379 (2009).
47. E. Shirzaei Sani, R. Portillo-Lara, A. Spencer, W. Yu, B. M. Geilich, I. Noshadi, T. J. Webster, N. Annabi, Engineering adhesive and antimicrobial hyaluronic acid/elastin-like polypeptide hybrid hydrogels for tissue engineering applications. *ACS Biomater. Sci. Eng.* **4**, 2528–2540 (2018).
48. N. Annabi, Y. N. Zhang, A. Assmann, E. S. Sani, G. Cheng, A. D. Lassaletta, A. Vegh, B. Dehghani, G. U. Ruiz-Esparza, X. Wang, S. Gangadharan, A. S. Weiss, A. Khademhosseini, Engineering a highly elastic human protein–based sealant for surgical applications. *Sci. Transl. Med.* **9**, eaai7466 (2017).

Acknowledgments

Funding: This work is supported by National Institutes of Health (NIH) (R01EB023052 and R01HL140618), the American Heart Association (AHA; 16SDG31280010), Department of Defense Vision Research Program Technology/Therapeutic Development Award (W81XWH-18-1-0654), Research to Prevent Blindness (RPB) Stein Innovation Award, and the Canadian Institutes of Health Research (CIHR). **Author contributions:** E.S.S., A. Khe., A. Kha., R.D., and N.A. designed the experiments. E.S.S. and A.S. synthesized the GelCORE. E.S.S., D.R., and A.S. conducted the physical characterization and adhesion experiments. E.S.S. and W.F. conducted the ex vivo burst pressure and retention tests. E.S.S. conducted the in vitro cytocompatibility and scratch test. A. Khe., E.S.S., Z.S., and W.F. conducted the in vivo experiments, and E.S.S. and Z.S. performed histopathological analysis. All the authors contributed to the interpretation of the results and data analysis. The paper was written by E.S.S. and D.R. and was revised and corrected by N.A., R.D., A. Kha., A. Khe., and A.S. The project was supervised by N.A. and R.D. **Competing interests:** R.D., A. Khe., A. Kha., and N.A. are inventors on a patent application related to this work filed by the Massachusetts Eye and Ear Infirmary and the Brigham and Women's Hospital Inc. (European Regional Phase Application no. EP17750660.7, from International Patent Application no. PCT/US2017/016917, based on U.S. Provisional Application no. 62/292,752). The other authors declare that they have no competing interests. **Data and materials availability:** All data needed to evaluate the conclusions in the paper are present in the paper and/or the Supplementary Materials. Additional data related to this paper may be requested from the authors.

Submitted 17 August 2018
Accepted 31 January 2019
Published 20 March 2019
10.1126/sciadv.aav1281

Citation: E. Shirzaei Sani, A. Kheirkhah, D. Rana, Z. Sun, W. Foulsham, A. Sheikhi, A. Khademhosseini, R. Dana, N. Annabi, Sutureless repair of corneal injuries using naturally derived bioadhesive hydrogels. *Sci. Adv.* **5**, eaav1281 (2019).

Science Advances

Sutureless repair of corneal injuries using naturally derived bioadhesive hydrogels

Ehsan Shirzaei Sani, Ahmad Kheirkhah, Devyesh Rana, Zhongmou Sun, William Foulsham, Amir Sheikhi, Ali Khademhosseini, Reza Dana and Nasim Annabi

Sci Adv **5** (3), eaav1281.
DOI: 10.1126/sciadv.aav1281